

SUPPLEMENTARY INFORMATION

miR-135a-5p-mediated downregulation of protein-tyrosine phosphatase delta is a candidate driver of HCV-associated hepatocarcinogenesis

Nicolaas Van Renne^{1,2}, Armando Andres Roca Suarez^{1,2}, Francois H. T. Duong³, Claire Gondeau^{4,5}, Diego Calabrese³, Nelly Fontaine^{1,2}, Amina Ababsa^{1,2}, Simonetta Bandiera^{1,2}, Tom Croonenborghs^{6,7}, Nathalie Pochet^{6,7}, Vito De Blasi^{1,2,8}, Patrick Pessaux^{1,2,8}, Tullio Piardi⁹, Daniele Sommacale⁹, Atsushi Ono^{10,11}, Kazuaki Chayama^{11,12,13}, Masashi Fujita¹⁴, Hidewaki Nakagawa¹⁴, Yujin Hoshida¹⁰, Mirjam B. Zeisel^{1,2}, Markus H. Heim³, Thomas F. Baumert^{1,2,8} and Joachim Lupberger^{1,2}

¹Inserm, U1110, Institut de Recherche sur les Maladies Virales et Hépatiques, ²Université de Strasbourg, Strasbourg, France, ³Department of Biomedicine, Hepatology Laboratory, University of Basel, Basel, Switzerland, ⁴Inserm, U1183, Institut de Médecine Régénératrice et Biothérapie, Université de Montpellier, Montpellier, France, ⁵Département d'Hépatogastroentérologie A, Hôpital Saint Eloi, CHU Montpellier, France, ⁶The Broad Institute of Massachusetts Institute of Technology and Harvard, Cambridge, MA, USA, ⁷Program in Translational NeuroPsychiatric Genomics, Brigham and Women's Hospital, Harvard Medical School, Broad Institute of Massachusetts Institute of Technology and Harvard, Cambridge, MA, USA, ⁸Pôle Hépat-Digestif, Institut Hospitalo-Universitaire, Hôpitaux Universitaires de Strasbourg, Strasbourg, France, ⁹Department of General, Digestive and Endocrine Surgery, Hôpital Robert Debré, Centre Hospitalier Universitaire de Reims, Université de Reims

Champagne-Ardenne, Reims, France, ¹⁰Division of Liver Diseases, Department of Medicine, Liver Cancer Program, Tisch Cancer Institute, Icahn School of Medicine at Mount Sinai, New York, USA. ¹¹Department of Gastroenterology and Metabolism, Applied Life Sciences, Institute of Biomedical & Health Sciences, Hiroshima University, Hiroshima, Japan, ¹²Laboratory for Digestive Diseases, RIKEN Center for Integrative Medical Sciences, The Institute of Physical and Chemical Research (RIKEN), Hiroshima, Japan, ¹³Liver Research Project Center, Hiroshima University, Hiroshima, Japan, ¹⁴Laboratory for Genome Sequencing Analysis, RIKEN Center for Integrative Medical Sciences, Tokyo 108-8639, Japan

Supplementary table S1: Human liver biopsies used in this study. NET= neuroendocrine tumor, gGT= gamma-glutamyl transferase, HCC= hepatocellular carcinoma, ASH= alcoholic steatohepatitis, FNH= focal nodular hyperplasia, PSC= primary sclerosing cholangitis, alcohol= alcohol abuse, AHT= arterial hypertension, SA= sleep apnea, COPD= chronic obstructive pulmonary disease, f= female, m= male, NA= not assessed.

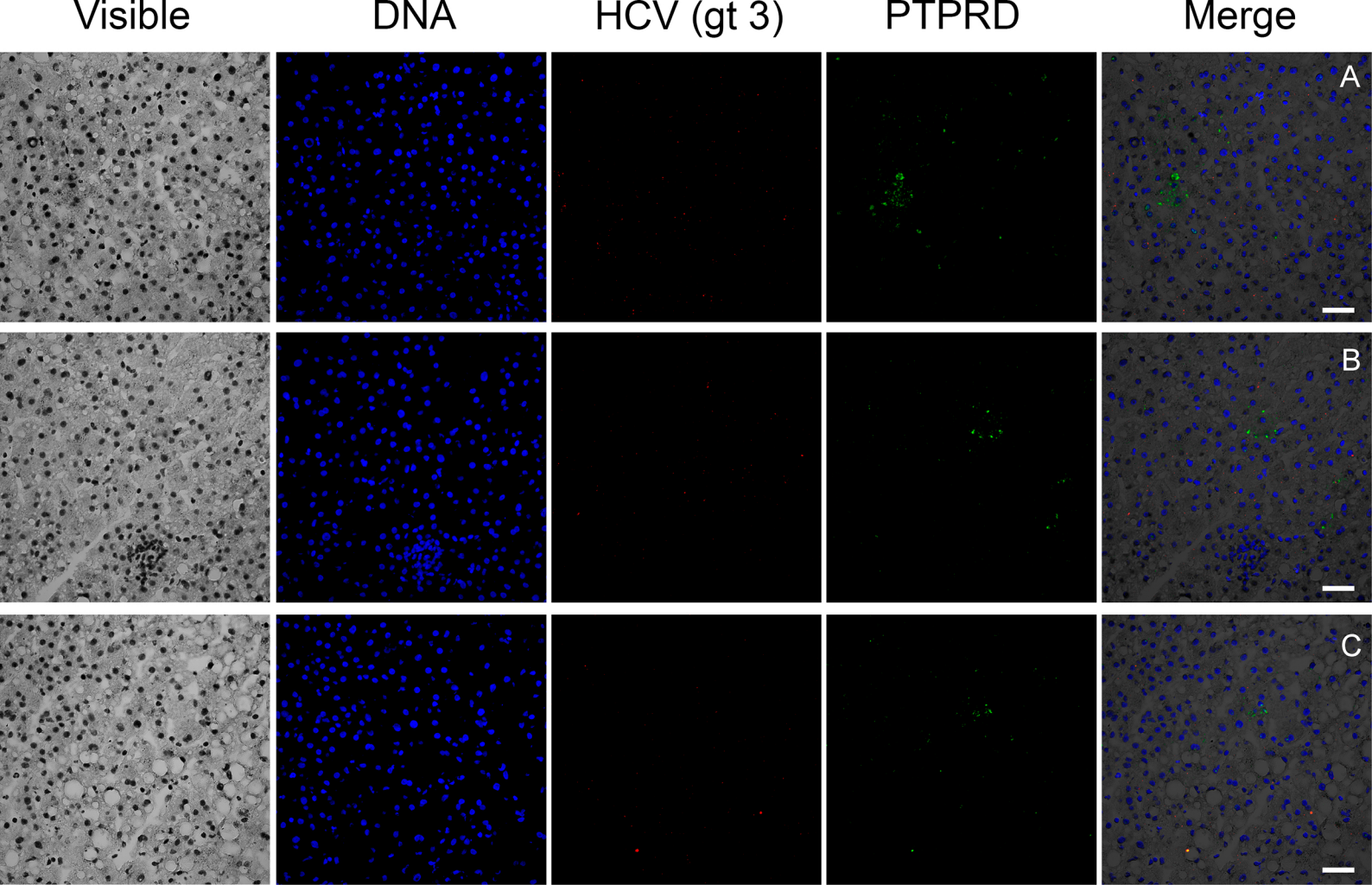
Figure	Code	Sex	Age	HCV <i>Genotype</i>	Viral load <i>IU/mL</i>	METAVIR	Diagnosis
1A	B318	f	78				NET, sample shows normal histology
1A	B724	m	66				Transaminase elevations
1A	B748	f	53				gGT and transaminase elevations
1A	B803a	m	69				Adenocarcinoma, sample shows normal histology
1A	B831	f	46				gGT elevations
1A	B895a	f	29				FNH, sample shows normal histology
1A,C-D	C32	m	59	1b	8.57E+05	A3/F2	HCV
1A,C-D	C12	m	53	4	3.31E+06	A2/F1	HCV
1A,C-D	C20	f	51	1a	NA	A1/F1	HCV
1A,C-D	C21	m	40	1a	NA	A1/F2	HCV
1A,C-D	C4	m	58	1b	3.21E+05	A3/F4	HCV
1A,C-D	C7	m	46	1a	4.33E+06	A3/F4	HCV
1B-D	C114	m	45	1a	1.17E+06	A1/F1	HCV
1B-D, 3	C121	m	65	2	5.89E+06	A2/F2	HCV

1B-D, 3	C124	f	48	3a	1.51E+06	A3/F4	HCV
1B-D, 3	C146	m	42	1a	NA	A2/F4	HCV
1B-D, 3	C149	m	34	3a	2.29E+04	A3/F4	HCV
1B-D, 3	C172	m	51	3a	3.47E+06	A2/F3	HCV
1B-D, 3	C221	m	34	3c	5.28E+05	A2/F4	HCV
1B-D, 3	C238	f	54	1b	NA	A1/F1	HCV
1B-D, 3	C239	m	52	NA	2.79E+05	A3/F4	HCV
1B-D, 3	C257	m	30	1a	1.08E+05	A1/F1	HCV
1B-D, 3	C263	f	62	3a	1.93E+05	A2/F1	HCV
1B-D, 3	C269	m	46	1a	1.62E+06	A2/F2	HCV
1B-D, 3	C270	f	76	1b	1.75E+06	A3/F3	HCV
1B-D, 3	C281	f	40	3a	NA	A1/F1	HCV
1B-D	C285	f	42	1a	2.80E+06	A1/F1	HCV
1B-D, 3	C291	m	53	3a	1.42E+05	A3/F2	HCV
1B-D, 3	C293	m	57	NA	NA	A3/F4	HCV
1B-D, 3	C300	m	55	3a	1.95E+06	A3/F4	HCV
1B-D, 3	C304	f	38	1a	1.55E+06	A2/F3	HCV
1B-D, 3	C44	f	41	1b	2.91E+05	A3/F4	HCV
1B-D, 3	C53	m	55	1b	2.17E+06	A2/F4	HCV
1B-D, 3	C58	m	54	4c/d	1.31E+06	A1/F1	HCV
1B-D, 3	C73	m	55	1b	2.62E+06	A3/F4	HCV
1B-D, 3	C89	m	29	3a	3.22E+04	A1/F1	HCV
1B-D, 3	C145	f	43				Normal
1B-D, 3	C187	f	31				Normal
1B-D, 3	C28A	f	51				Normal
1B-D, 3	C29	m	62				Normal
1B-D, 3	C305	m	46				Minimal unspecific hepatitis
1B-D, 3	C330	m	47				Minimal steatosis
1B-D, 3	C366A	f	56				Normal
1B-D, 3	C369	m	37				Normal
1B-D, 3	C442A	m	69				Minimal reactive hepatitis, 10 % steatosis
1B-D, 3	C445	m	33				Normal
1B-D, 3	C51A	f	55				Normal
1E	B229	m	37	3a	8.3E+05	A2/F3	HCV
1E	B512	m	44	3a	2.4E+04	A2/F2	HCV
1E	C37	f	51	3a	8.5E+06	A2/F1	HCV
5A	C126	m	81				HCC, ASH, cirrhosis
5A	C127	m	66				HCC, ASH, cirrhosis
5A	C133	m	67				HCC
5A	C65	m	77				HCC, ASH, cirrhosis
5A	C66	m	72				HCC, ASH, cirrhosis
5A	C78	f	57	3a	2.8E+04	A2/F4	HCV, HCC, cirrhosis
S6-7	14B04331	m	60			F3	Diabetes, alcohol
S6-7	14B04479	m	80			F3	Alcohol
S6-7	14B04674	m	65			F4	Diabetes, alcohol
S6-7	14B05087	m	63			F4	Diabetes, alcohol, HBV

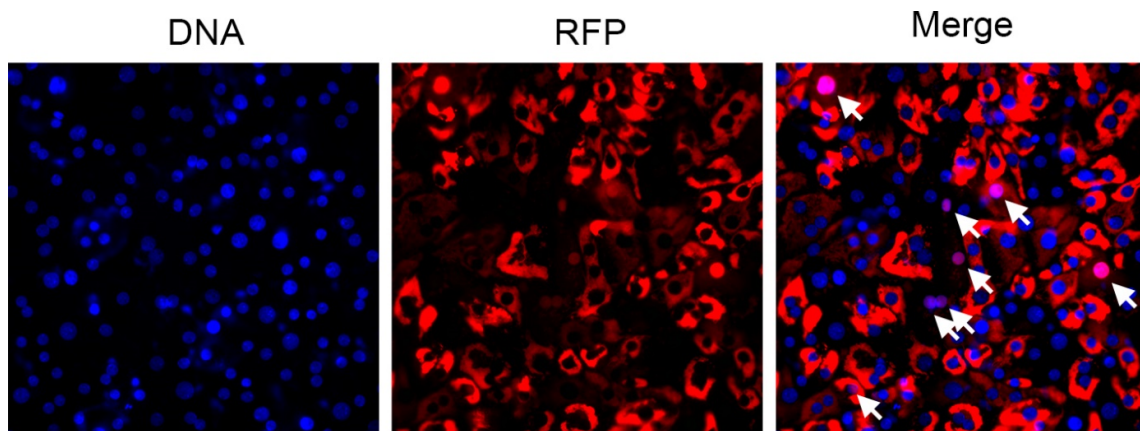
S6-7	14B05224	m	63			F4	Alcohol
S6-7	14B05345	m	72			F4	Alcohol
S6-7	14B05732	m	54	1b		F4	HCV, alcohol
S6-7	14B06994	m	66			F0	
S6-7	14B07954	m	74			F3	Diabetes
S6-7	14B08723	f	68			F2	
S6-7	15B00027	m	65			F4	HBV
S6-7	15B00395	m	64			F3/4	Alcohol, HBV
S6-7	15B00147	m	58			F4	Diabetes, alcohol
S6-7	15B00738	m	64			F3/4	Alcohol
S6-7	15B00971	m	81			F4	
S6-7	15B01490	m	54	1b		F4	HCV, diabetes
S6-7	15B01592	f	54	1b		F4	HCV
S6-7	15B02140	f	71			F0	
S6-7	15B02690	m	70	1b		F3	HCV
S6-7	15B03066	f	57			F4	Diabetes, alcohol
S6-7	15B04170	m	72			F4	Alcohol
S6-7	15B05646	m	75			F2	Diabetes
S6-7	15B05842	m	67			F4	Alcohol
S6-7	15B06370	m	66			F0	
S6-7	15B06514	m	65			F4	Alcohol
S6-7	16B00429	m	60			F0	Alcohol
S7	2065512	m	75				Alcohol, AHT, diabetes, dyslipidemia, obesity
S6-7	1369075	m	69				Alcohol, AHT, diabetes, dyslipidemia, obesity
S6-7	0020219	m	67				AHT, PSC
S6-7	1066280	m	70				AHT, arteriopathy
S6-7	1501765	m	80	1b		A2/F2	HCV
S6-7	2099524	m	71				Alcohol, obesity, AHT, dyslipidemia
S6-7	0099746	f	56	3a		A0/F2	HCV, obesity, AHT
S6-7	0644778	m	46	3a		A0/F2	HCV, AHT, alcohol
S6-7	1111249	m	57				Obesity, alcohol
S6-7	0320724	m	64				Obesity, diabetes, AHT
S6-7	1514711	m	57				AHT, diabetes
S6-7	1830303	m	50	3a		A2/F4	HCV, alcohol
S6-7	1164689	m	58	1a		A0/F2	HCV
S6-7	0211312	m	54	1a		A0/F4	HCV
S6-7	1450114	m	72				COPD, diabetes, AHT, SA, dyslipidemia
S6-7	1932776	f	65	1b		A2/F2	HCV, AHT, depression, vasculopathy
S6-7	0659735	f	70	1b		A1/F1	HCV, AHT, alcohol, vascular injury, COPD, osteoporosis
S6-7	0730036	m	60				Diabetes, AHT

Supplementary table S2: miRNA expression in Huh7.5.1 cells infected with HCVcc and in human liver biopsies from HCV infected patients. miRNAs that are upregulated by HCVcc (strain Jc1) in undifferentiated Huh7.5.1 cells and that are predicted to target the 3' untranslated region (3'UTR) of the PTPRD mRNA. miRNA targeting prediction was performed using the following tools incorporated in the miRSystem database [1]: a= DIANA, b= MIRANDA, c= MIRBRIDGE, d= PICTAR, e= PITA, f= TARGETSCAN. fc= fold change, p-values (U-Test, n=33) correspond to miRNA expression levels in liver biopsies.

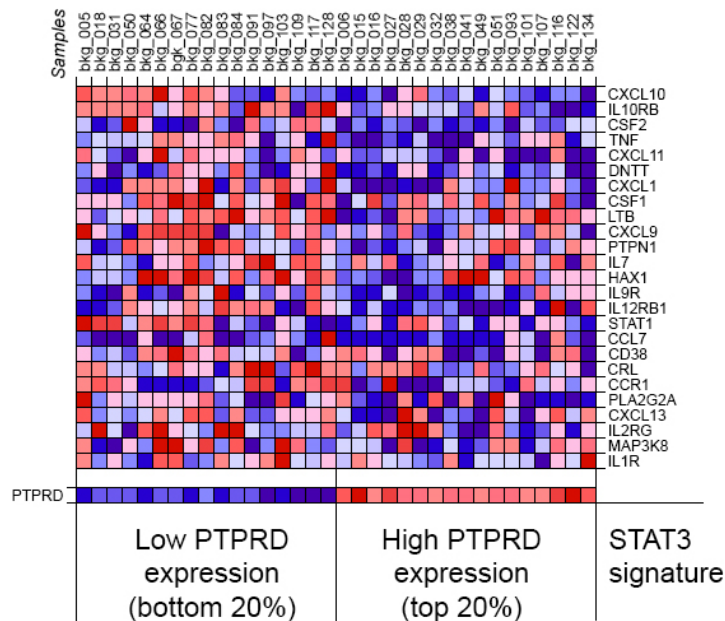
miRNA	ID (MIMAT)	Target sites on 3'UTR	Predicted by (tools)	Expression in HCVcc-infected Huh7.5.1 (fc)	Expression in HCV(+) liver biopsies (median fc)	U-test (p)
miR-16-5p	0000069	1	a,b,c,e,f	1.62	1.03	0.90
miR-24-3p	0000080	1	a,b,c,d,e,f	1.34	1.33	0.59
miR-26a-5p	0000082	1	a,b,c,e,f	2.77	1.03	0.64
miR-29a-3p	0000086	1	a,c,f	1.70	1.28	0.19
miR-29b-3p	0000100	1	a,c,f	1.49	1.13	0.94
miR-135a-5p	0000428	2	a,b,d,e,f	2.09	2.51	6E-04
miR-148a-3p	0000243	1	a,b,c,e,f	2.00	-1.34	0.04
miR-194-5p	0000460	1	a,b,c,e,f	6.39	-1.05	0.40



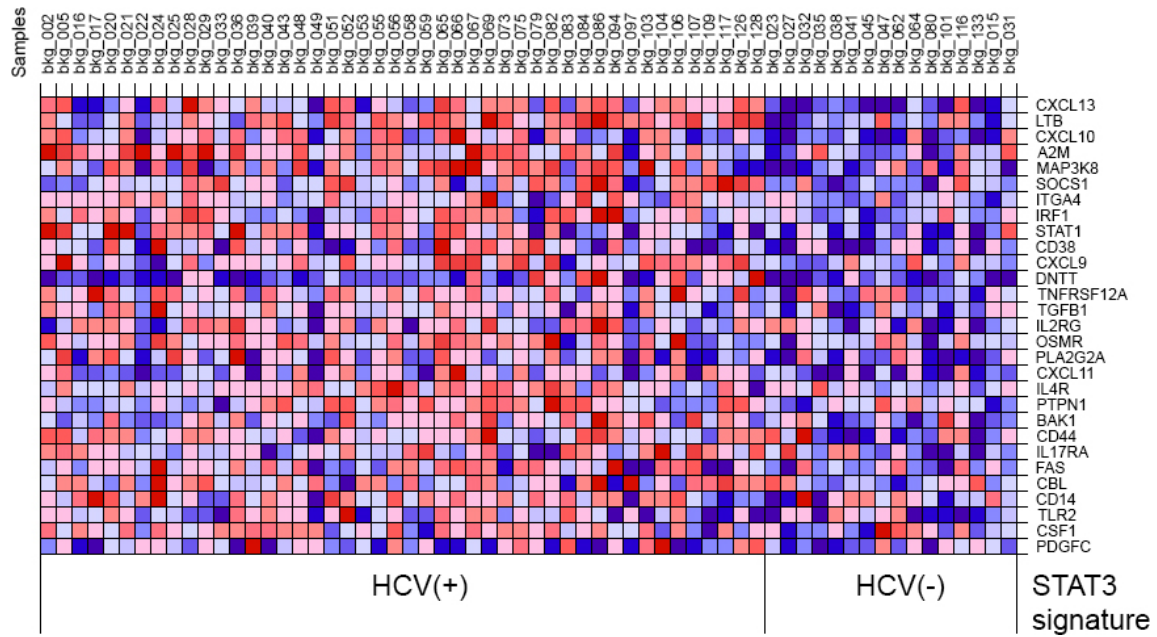
Supplementary figure S1: PTPRD expression is impaired in HCV-infected hepatocytes in liver biopsies. Representative images from FISH analysis of three different liver biopsies infected with HCV by simultaneous hybridization with HCV-specific and PTPRD-specific probe sets. **(A)** Liver biopsy B229, **(B)** liver biopsy B512, **(C)** liver biopsy C37; Grey= visible light channel, blue= genomic DNA, red= HCV RNA genotype 3, green= PTPRD RNA, scale bar= 100 μm .



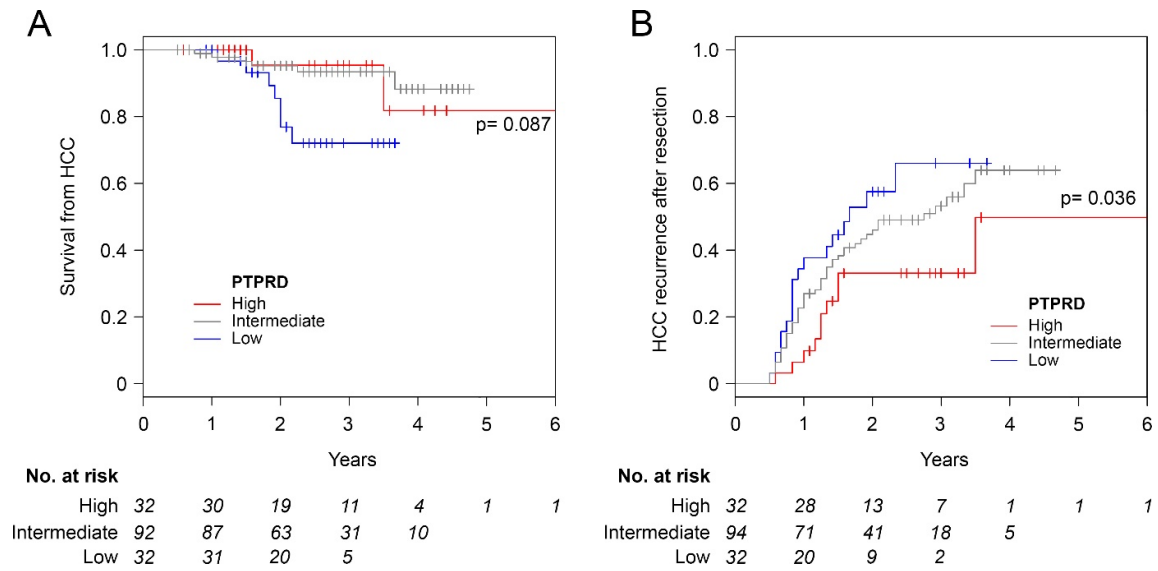
Supplementary figure S2: HCV infection of primary human hepatocytes *ex vivo*. Representative image of a RFP-NLS-IPS HCV infection reporter assay [2] from an independent experiment. Primary human hepatocytes were transduced with lentiviruses expressing RFP-NLS-IPS at day 1 post-seeding and then were inoculated with HCVcc (strain JFH1). HCV-infected cells were identified by translocation of the cleavage product RFP-NLS to the nucleus (pink nuclei indicated by arrows) 72 h post-infection. Image magnification 40x.



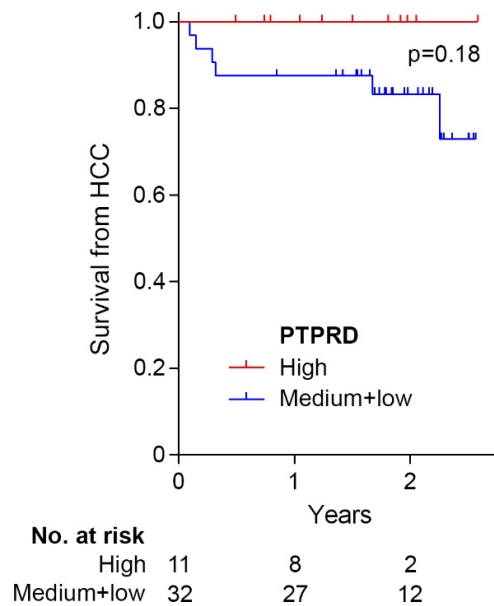
Supplementary figure S3: A gene expression signature responsive to STAT3 transcriptional activity is enhanced in liver biopsies with intermediate/low PTPRD expression. *In silico* analysis of mRNA expression in liver biopsies adjacent to HCC lesions [3]. Enrichment of the Hallmark_IL6 JAK STAT3 signaling transcriptional program (STAT3 signature) [4] clustered with the 20 % liver biopsies with lowest PTPRD mRNA expression. 25 of 78 leading edge genes of the STAT3 signature contributing to the enrichment score shown in Fig. 4C. High PTPRD expression corresponds to the top 20 % percentile of biopsies measured, low PTPRD expression corresponds to the 20 % percentile with lowest PTPRD expression of all assessed liver biopsies in Fig. 4B (Supplementary table S1). Red= high mRNA expression, blue= low mRNA expression.



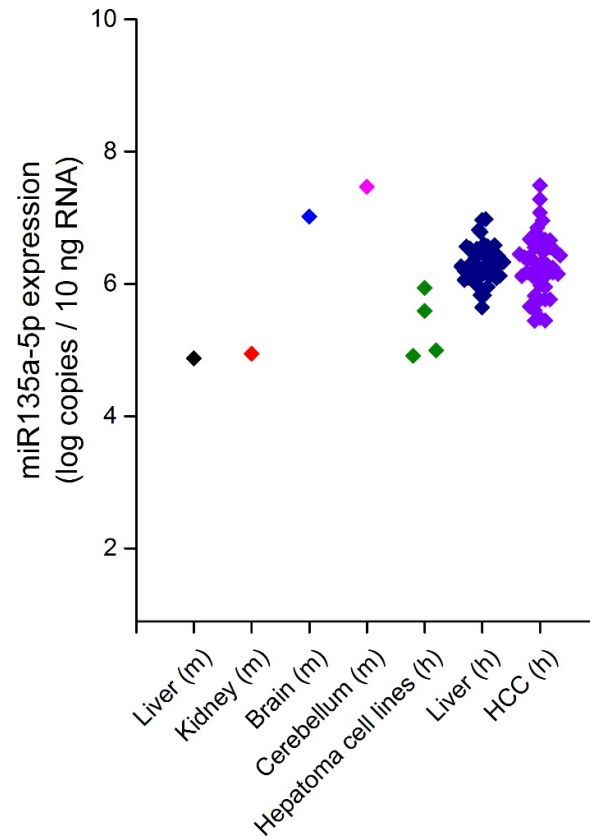
Supplementary figure S4: A gene expression signature responsive to STAT3 transcriptional activity is enhanced in liver biopsies of HCV-infected patients. *In silico* analysis of an mRNA expression database [3]. Enrichment of the STAT3 transcriptional program clusters in HCV-infected biopsies (HCV(+), n=46) vs. confirmed HCV negative biopsies (HCV(-), n=16). 29 of 78 leading edge genes from the Hallmark_IL6 JAK STAT3 signaling gene set (STAT3 signature) [4] were contributing to the enrichment score shown in Fig. 4E. Red= high mRNA expression, blue= low mRNA expression.



Supplementary figure S5: Low PTPRD expression in liver biopsies is associated with a decreased patient survival from HCC and elevated HCC recurrence after surgical resection in cohort B. Patients with low PTPRD expression in adjacent non-tumor tissues are associated with decreased survival from HCC ($p=0.087$, log-rank test) after a follow-up of 6 years. Cohort B comprises 158 patients with HCC from the Hiroshima University Hospital, Japan. Product-limit estimation of PTPRD expression in adjacent non-tumor tissue compared with disease progression data from patients. **(A)** Probability of overall survival after surgical resection according to PTPRD expression levels **(B)** Probability of HCC recurrence after surgical resection according to PTPRD expression levels. Data were analyzed using Kaplan-Meier estimator. Number of patients at risk (No. at risk) are indicated.



Supplementary figure S6: High PTPRD expression in liver biopsies is potentially associated with an elevated patient survival from HCC in cohort C. Patients with high PTPRD expression in adjacent non-tumor tissues exhibit a trend of increased survival from HCC ($p=0.18$, log-rank test) after only 2 ½ years of follow-up. Cohort C comprises 44 patients with HCC from the University Hospitals of Strasbourg and Reims, France. One patient was omitted from the analysis due to perioperative mortality. Product-limit estimation of PTPRD expression in adjacent non-tumor tissue of 43 patients compared with disease progression data from patients. Because of the short follow-up period patient survival from HCC was compared between biopsies with highest PTPRD expression (top 25 %) and biopsies exhibiting medium to low PTPRD expression (75 %) using Kaplan-Meier estimator (Software GraphPad Prism 6). Number of patients at risk (No. at risk) are indicated.



Supplementary figure S7: Tissue expression of miR-135a-5p. miR-135a-5p is expressed in liver tissue from both mouse and human. The sequences of miR-135a-5p in mouse (mmu-miR-135a-5p) and human (hsa-miR-135a-5p) are identical. miR-135a-5p expression was analyzed by RT-qPCR in mouse-derived tissues (liver, kidney, brain and cerebellum) and human liver specimens from cohort C (n=44) including HCC resections and adjacent liver tissues (Supplementary table S1, Fig. S6). Dilutions of synthetic miR-135a-5p mimic RNA served as standard for the miR-135a-5p quantification.

Supplementary references

- 1 Lu TP, Lee CY, Tsai MH, Chiu YC, Hsiao CK, Lai LC, *et al.* miRSystem: an integrated system for characterizing enriched functions and pathways of microRNA targets. *PLoS One* 2012;**7**:e42390.
- 2 Kim HY, Li X, Jones CT, Rice CM, Garcia JM, Genovesio A, *et al.* Development of a multiplex phenotypic cell-based high throughput screening assay to identify novel hepatitis C virus antivirals. *Antiviral Res* 2013;**99**:6-11.
- 3 Hoshida Y, Villanueva A, Kobayashi M, Peix J, Chiang DY, Camargo A, *et al.* Gene expression in fixed tissues and outcome in hepatocellular carcinoma. *N Engl J Med* 2008;**359**:1995-2004.
- 4 Liberzon A, Birger C, Thorvaldsdottir H, Ghandi M, Mesirov JP, Tamayo P. The Molecular Signatures Database (MSigDB) hallmark gene set collection. *Cell Syst* 2015;**1**:417-25.